7-10-1995

Stability of Growing Front of YBa(2)Cu(3)O(x) Superconductor in the Presence of Pt and CeO(2) Additions

Gregory Kozlowski
Wright State University - Main Campus, gregory.kozlowski@wright.edu

Tom Svobodny
Wright State University - Main Campus, thomas.svobodny@wright.edu

Stability of growing front of $YBa_2Cu_3O_x$ superconductor in the presence of Pt and CeO_2 additions

Gregory Kozlowski and Thomas Svobodny
Wright State University, Dayton, Ohio 45435

(Received 9 December 1994; accepted for publication 21 April 1995)

Distinctive microstructures of textured $YBa_2Cu_3O_x$ (123) superconductors were examined by scanning electron microscopy and metallurgical microscopy. The samples were synthesized under a residual thermal gradient by using a modified melt textured growth on a Y_2BaCuO_5 (211) substrate. Also, the unidirectional solidification by a zone-melting method was performed to fabricate 123 superconducting bars up to 12 cm long placed on the 211 substrate in the horizontal arrangement, with a growth rate $R=0.5$ mm/h and a temperature gradient of $G=20$ °C/cm ($G/R=400$ °C h/cm^2). A ramping temperature of 1 °C/h (GR) was applied in both syntheses. Typical defects running parallel to (001) planes associated with 211 trapped particles were observed (so-called platelet structure). Besides these, unusual defects were observed running parallel to (100) and (010) planes in textured 123+Pt superconductors, and interpreted as the result of an instability of the planar front in the presence of fine 211 particles. A theoretical model of planar interface stability confirms a strong dependence of stability region on the size of 211 particles in the melt. © *1995 American Institute of Physics.*

The three-dimensional planar front of the 123 crystal with large anisotropy is determined, under steady state conditions, by the (100), (010), and (001) faces. These crystals usually need a large undercooling to establish the planar growth front. It is accepted[1] that the *F* faces [e.g., (001)] and the *S* faces [e.g., (100) and (010)] constitute the structural morphology of the 123 crystal. An *F* face grows according to a layer growth mechanism in a spiral pyramid in contrast to the *S* face which grows according to one-dimensional nucleation. As a result, the *F* face grows more slowly than the *S* face and should form the planar front with the (001) and (011) faces. The appearance of the (100) and (010) faces instead of the (011) face may be ascribed to factors such as face-specific adsorption of liquid at the planar front, the existence of 211 particles in the vicinity of the front, and entrapment of 211 particles by the 123 crystal.[2] It is known that the textured 123 superconductor is a defective crystal with growth induced defects (low-angle boundaries) containing traces of trapped liquid.[3] These defects are parallel to the (001) planes and they are associated with 211 trapped particles. Precipitate formation in the trapped 211 particles and yttrium enrichment of 123 close to the planar front agrees with the crystallization of superconductor directly from an undercooled melt. When the planar front meets 211 particles, it pushes them if the particles are smaller than a critical radius.[4] Larger 211 particles are trapped by the interface and the planar front engulfs these particles leaving behind gaps (or growth-induced defects) from 100 to 1000 nm wide and filled with the liquid rich in barium and copper oxides. Transmission electron microscopy (TEM)[3] reveals that these gaps between the ledges of the 123 matrix show a toothlike structure. The tooth direction is perpendicular to the growth direction with the tooth lying along the (001) planes. This picture of crystal growth is indicative of instability in the planar front.

There is already well-known evidence to underline the importance of finer 211 particles in the morphology of crystal growth of 123 with Pt, CeO_2, and PtO_2 additions and the effect of these particles on the critical current density. First, it has been shown[5] that the maximum growth rate at which a planar front solidification can be sustained is inversely proportional to the 211 particle size. Second, several groups have attributed the 211 refinement to a decreasing chemical potential gradient and/or a change in diffusivity in the liquid phase and/or a reduction in the surface energy between 211 and the melt. The segregation of the 211 particles in the form of tracks in PtO_2 doped 123 was observed in Ref. 6. This should be related to the initial morphology of the 211 particles, just subsequent to the peritectic decomposition reaction. And finally, the smallest 211 particles may also induce a different kind of relaxation mechanism. Microstructural studies including TEM[3] have shown the extended perturbation of the matrix (up to 4 μm) due to the relaxation of a higher surface energy of these 211 particles. Also, these smaller particles appear to have a defective chemical composition associated with a strongly deformed structure.

The present study is concentrated on an understanding of what effect Pt or CeO_2 additions have on the morphology of the planar front solidification in the melt-textured 123.

All of the experiments in this study use commercially available 123 powder (2–5 μm particle size) supplied by SSC, Inc. A Pt powder (of 99.99% purity), supplied by Johnson-Mathey Co., was mixed with 123 in the proportion of 0.1, 0.3, and 0.5 wt% using a mortar and pestle. Both doped and undoped pellets (4 g each) and bars (12 or 24 g each) were prepared. These samples rested on high-density (5.7 g cm^{-3}) 211 substrates that matched in shape and whose weight was four times smaller than the respective samples. One set of samples was inserted in a preheated box furnace at 1100 °C, held for 0.2 h after the temperature stabilized, and was then slowly cooled at a rate of 1 °C/h from 1015 to 925 °C followed by a fast cooling at a rate of 240 °C/h to

 0003-6951/95/67(2)/288/3/$6.00

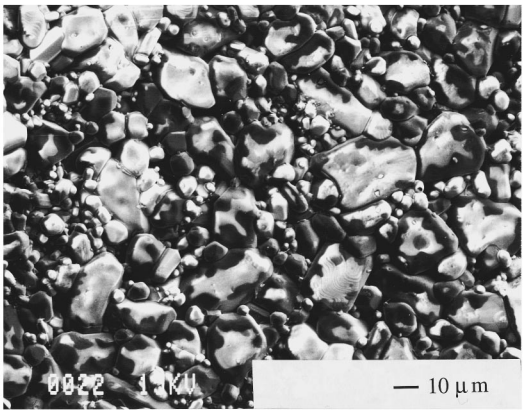

FIG. 1. SEM micrograph of 211 substrate used in melt process.

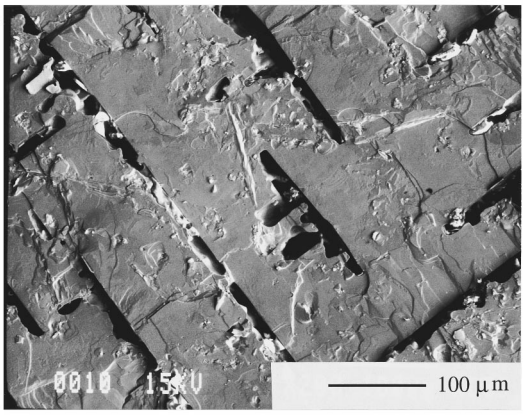

FIG. 3. Typical morphology of 123+Pt single crystal grown by using modified melt-textured technique or zone-melting method.

reach room temperature (modified melt-texture growth). A second set of bars (12 and 24 g in weight and up to 12 cm long) were unidirectionally solidified by a zone-melting method on the 211 substrate in the horizontal arrangement, with a growth rate of $R=0.5$ mm/h with a temperature gradient of $G=20$ °C/cm. The processed samples on the polycrystalline substrate of 211 (Fig. 1) show a high texturation (Fig. 2) with and without temperature gradient. Similar experiments with CeO_2 additions were also carried out. It is important to note that: (i) the use of the high-density substrate substantially reduces the reaction between the 123 pellet and the substrate, and (ii) a stoichiometric imbalance of more than 2.5 wt% 211 will not produce the distinctive microstructure observed here.

Figure 2 displays a sample sliced along a (001) plane. One clearly sees nonsolidified linear recesses of 10–20 μm in width and spaced about 100 μm apart. (We will refer to the part of the crystal between the recesses as an arm.) The arms extend in the [100] and [010] directions, that is, the ''V'' points in the [110] direction. In the arms, the platelets can be seen parallel to (001). The recesses or gaps contain $BaCuO_2$ and CuO; these can be seen as a whitish residue in Fig. 3. Along the [110] diagonal are distributed 211 particles of size 1–5 μm. A pregrowth distribution of 211 particles can be seen on the backsides of the arms. The dominant size is about 2 μm. The distribution of 211, as one moves through the arm toward the front, shows a marked decrease in the size of the particles.

A physical explanation for the size distribution can be arrived at by considering the mechanics of crystal growth. A (001) face grows via a spiral mechanism. The corners of the spiral correspond to the directions of fastest growth, in this case the [011]. Thus, in a local picture (a frame of reference moving with the front, which is, of course, not a material frame) the corner asserts itself like the prow of a ship. The smaller particles will be moved by the boundary layer in the melt, while the more massive particles will not be so affected, in accordance with the theory of Ref. 4. In fact the larger particles will be swallowed by the moving edge of the spiral; having been incorporated into the solid they will no longer dissolve but retain their size; meanwhile, the smaller particles that are pushed by the front will continue to supply the front with the necessary nutrient. The mechanism outlined here requires a certain heterogeneity in the sizes of the 211 particles. This heterogeneous distribution could result when the initial specimen, after the peritectic decomposition reaction, has needlelike 211 particles. In the subsequent melt, there will be a wide variety in the sizes of the 211 particles, due to pinching, etc.

The structure seen in Figs. 2 and 3 is not seen when the crystal is grown in the same way but without platinum. It has been conjectured that the structure observed in the presence of platinum may be due to liquid flux trapped in crystal because of increased liquid surface tension. For example, Ref. 7, a melt process of a series of 123 pellets placed on 211 substrates shows that the amount of liquid gained by the substrate decreases 50% when the pellets contain a small amount of Pt. The following experimental facts indicate that we cannot find an explanation of the observed morphology. A crystal with some substitution of holmium for yttrium was grown ($Y_{0.8}Ho_{0.2}Ba_2Cu_3O_x$) without platinum addition and the trapped liquid was found to be comparable to 123 with platinum; however, a smooth growth structure is obtained without the periodically interrupted growth shown in the illustrations accompanying this letter. If one then grows $Y_{0.8}Ho_{0.2}Ba_2Cu_3O_x$ with platinum added, then, once again, the interrupted growth front is seen.[7] The key observation, in our view, is the spatial distribution of 211 particle size.

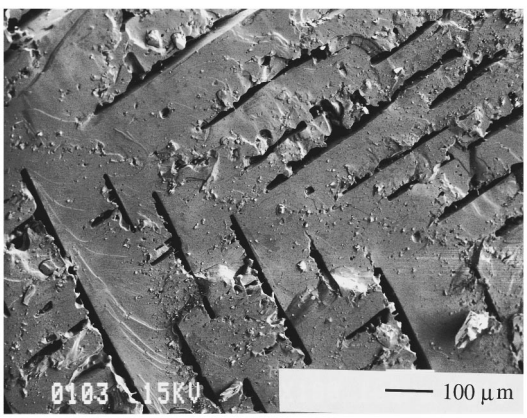

FIG. 2. Fracture surface micrograph of melt process 123+Pt sample.

Larger particles are found along the joint of the arms and on the backside of the arms, smaller particles at the stagnated front of the arm. This experimental picture, coupled with some results of Ref. 3 who found evidence of supersaturation at all times at the growing front, so that the stagnation is not due to yttrium deficiency, strongly suggests that morphological instability plays an important role. It is believed that the effect of the additions is to reduce surface energy of the 211 particles in the pregrowth melt, resulting in a characteristic needlelike shape of the particles. The needlelike shape of the 211 inclusions is implicated indirectly; the direct influence in this mechanism is the heterogeneity of the size distribution.

We have calculated the effect of the varying size of 211 inclusion on the growth of small amplitude disturbances to the planar front. The main assumption in the analysis is that the particle size l is directly related to the interparticle distance. This allows us to set up a boundary value problem for the steady state diffusion of yttrium from solid 211 through the liquid to feed the growing 123 front. The full details of the mathematical analysis will be reported elsewhere. The results of this stability analysis show that the disturbance growth rate σ for a disturbance of wave number ω has a dependence on l of the following form

$$\sigma = 2V\omega\left(\frac{(-T_m\Gamma\omega^2 - G_1)(\Omega + G_c/C_\gamma^L) + m(\Omega - V/D)}{2\omega m + G_2(\Omega + G_c/C_\gamma^L)}\right),$$

where

$$\Omega = V/2D + (\Delta\omega/2)\coth(l\Delta\omega/2).$$

V is the velocity of the growing front, m is liquidus slope, and G_1, G_2 are thermogradient quantities; C_γ^L is the yttrium concentration at the growing front; C_α^L is the yttrium concentration at the liquid/211 boundary; T_m is the melt temperature; Γ is the capillary length; $G_c = l_d^{-1}(C_\alpha^L - C_\gamma^L)[1 - \exp(-l/l_d)]^{-1}$, and $\Delta\omega = 2\sqrt{(2l_d)^{-2} + \omega^2}$. Note that the growth relation reduces to the usual Mullins–Sekerka formula for large l. For l not significantly less than the diffusion length, $l_d = D/V$, the stability region increases with decreasing l. Things are different, however, for very small l (small compared to l_d); in that case, we see that the growth rate is

$$\sigma \simeq 2V\omega\left(\frac{-(T_m\Gamma\omega^2 + G_1) + m}{2\omega m l + G_2}\right).$$

From this we draw two important conclusions. First, the region of stability does not continue to increase for small l; in fact, as l decreases, this region at some point increases, and for very small l, the marginally stable wave number, ω_c, does not change significantly for decreasing l. Second, there is another important length scale, $l_p = G_2/2m\omega_c$, and as l approaches this length from above, the growth rate increases as $\sim 1/l$ (Fig. 4). Using published values, we calculate that $\omega_c \approx 10^5$ cm^{-1} and so $l_p \approx 10^{-9}$ cm. We note that the size of the platelets observed in Fig. 2 is in the range between l_p and l_d.

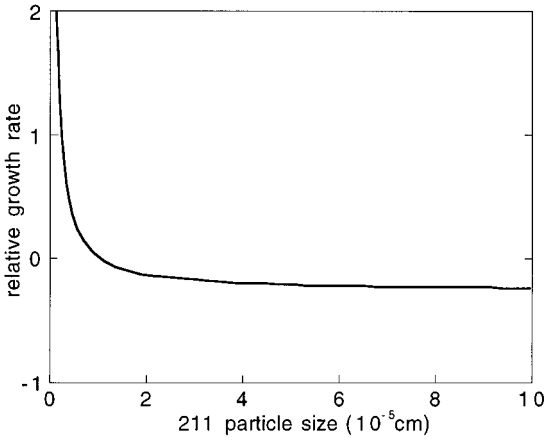

FIG. 4. Typical dependence of the growth rate of planar front on size of 211 particle. Here, the wave number is 10 000 cm^{-1}.

We believe the above considerations lend credence to the idea that an instability, in a yttrium-supersaturated growing front, in the presence of small size 211 particles, is the mechanism for the observed structures in textured 123. The importance that these seemingly peculiar structures may have to the problem of bulk transport currents in 123 will be detailed elsewhere.

One of the authors (G.K.) wishes to acknowledge Dr. C. Oberly for the provision of laboratory facilities, and the Air Force for financial support.

[1] B. N. Sun, P. Hartman, C. F. Woensdregt, and H. Schmid, J. Cryst. Growth **100**, 605 (1990).
[2] Y. Nakamura, K. Furuya, T. Izumi, and Y. Shiohara, J. Mater. Res. **9**, 1350 (1994).
[3] J. Ayache, P. Odier, and N. Pellerin, Supercond. Sci. Technol. **7**, 655 (1994).
[4] D. R. Uhlmann, B. Chalmers, and K. A. Jackson, J. Appl. Phys. **35**, 2986 (1964).
[5] M. J. Cima, M. C. Flemings, A. M. Figueredo, M. Nakade, H. Ishii, H. D. Brody, and J. S. Haggerty, J. Appl. Phys. **72**, 179 (1992).
[6] C. Varanasi and P. J. McGinn, Physica C **207**, 79 (1993).
[7] G. Kozlowski (unpublished results).